Advances in Environmental Technology 12(3) 2026, 256-273.

Iranian Reasearch Organization for Science and Technology (IROST)

Advances in Environmental Technology

Journal home page: https://aet.irost.ir

Metal-organic framework based on iron doping: Green synthesis and sustainable adsorbent for anionic dye contaminated water

Reza Soleimani[a], Bayramali Mohammadnezhad[b]*, Seyed Abbas Hosseini[a]

[a] *Department of Civil Engineering, Science and Research Branch, Islamic Azad University, Tehran, Iran.*

[b] *Department of Civil Engineering, Faculty of Technical Engineering, Qom University of Technology (QUT), Qom, Iran.*

ARTICLE INFO

Document Type:
Research Paper

Article history:
Received 13 October 2025
Received in revised form
28 December 2025
Accepted 21 April 2026

Keywords:
Wastewater treatment
MOF
Dye Removal
Direct red 23
Green synthesis

ABSTRACT

Industrial effluents have emerged as a critical environmental challenge due to limited water resources, their toxic nature, and carcinogenic properties. Therefore, it is essential to treat industrial wastewater and eliminate toxic pollutants. This study focuses on synthesizing nanocrystals of zeolite imidazole frameworks (ZIF-8) by doping with iron to create a porous ZnFe/ZIF-8 (ZFZ) composite using a green method (water solvent) to enhance performance and synergistic effects. The morphology of ZFZ nanocrystals was analyzed using a variety of complementary characterization techniques (Fourier Transform Infrared (FTIR), X-ray diffraction (XRD), and scanning electron microscope (SEM)). The ZFZ and ZIF-8 were assessed for the removal of Direct Red 23 (DR-23) dye from wastewater by varying the effective variables (pH, dye dosage, initial concentration, an(d contact time). For comparative analysis, ZIF-8 was also synthesized and used in conjunction with ZFZ to remove the DR-23 dye. The results demonstrated that ZFZ possesses a significantly higher adsorption capacity (383 mg/g) for DR-23 than ZIF-8 (94.79 mg/g), representing a fourfold enhancement. At a contact time of 120 minutes, the ZFZ composite achieved a maximum removal efficiency of 92.3% with 0.006 g of adsorbent at pH 3. Analysis of the equilibrium adsorption data for anionic dyes confirmed a strong alignment with the Langmuir model (R^2 = 0.99), consistent with a homogeneous, monolayer adsorption process. Additionally, the adsorption mechanism on ZFZ and ZIF-8 composites followed second-order kinetics with R^2 = 0.99. These findings confirm that synthesized ZFZ is an efficient adsorbent for the remediation of dye-contaminated wastewater.

*Corresponding author Tel.: +98 912 2162060
E-mail: mohammadnezhad@qut.ac.ir
DOI: 10.22104/aet.2026.7493.2087

1. Introduction

Water resources are vital for all life, yet they face considerable challenges today due to industrial pollutants. The rapid expansion of industrial factories across various sectors has led to effluents and pollution of both surface and groundwater, constituting a significant threat to the sustainability of society and other species [1, 2]. Produced wastewater mainly contains polycyclic aromatic hydrocarbons and volatile organic compounds [3]. Common contaminants include heavy metal ions, phenols, pesticides, herbicides, fertilizers, hydrocarbons, detergents, industrial effluents, pharmaceutical active compounds, and organic dyes [4-6]. Organic dye contamination in water resources is concerning due to the dyes' chemical stability and resistance to degradation, which can cause genetic mutations and cancer in humans and harm the environment [7]. Organic pollutants and azo dyes are among the most pressing environmental concerns globally due to their toxicity and persistence in wastewater. Removal methods include adsorption, photocatalysis, coagulation-flocculation, ultrafiltration, and other chemical and membrane processes, each with limitations such as the production of toxic secondary pollutants and economic challenges [8]. Currently, adsorption is a leading wastewater treatment method due to its practicality, simple design, affordability, and environmental sustainability, attracting significant interest from scientists across various industries [9]. For instance, Azizi et al. demonstrated the effective use of a modified graphene oxide adsorbent to remove Direct Red 81, achieving high removal efficiencies and notable reusability [10].

Membrane processes, such as nanofiltration (NF), also present a viable alternative, particularly for ionic dyes. Askari et al. studied the decolorization of Reactive Blue 19 and Acid Black 172 using a polyamide NF membrane, achieving high removal efficiencies of up to 97% and 94%, respectively, at optimized conditions and highlighting NF as a lower-pressure alternative to reverse osmosis [11].

Metal-Organic Frameworks (MOFs) are highly porous, crystalline materials characterized by large structures composed of metal ions and organic linkers, forming scaffold-like architectures through coordination bonds [12]. Due to their diverse and regular structures, chemical stability, and robust mechanical strength, MOFs have rapidly gained attention across various scientific fields. Their extensive surface area, ultra-high porosity, and uniform pore dimensions, as well as adjustability, flexibility, and suitable selectivity, make them a viable alternative to other adsorbents [7, 13]. Over the last decade, MOFs have demonstrated promise in sensing, catalysis, separation, drug delivery, gas storage, and adsorption. Although extensive research exists on MOF development and applications, recent interest has focused on MOF composites with sodalite structures as hybrid templates and their complexes with various metals [14-17]. Among these, Zeolite imidazolate frameworks (ZIFs), a prominent subclass of MOFs featuring a zeolitic topology, have garnered significant attention. ZIFs, containing metal ions like Fe, Cu, Co, and Zn linked by imidazolium bonds (M-Im-M), exhibit characteristics of both zeolites and MOFs. Their substantial surface area, adjustable size, crystal structure, unimodal micropores, abundant functionality, and chemical and thermal stability make them excellent substrates for dye adsorption [3, 18].

Recently, hybrid MOFs incorporating metal complexes with unique structural capabilities have garnered significant scientific interest. Combining metals in the synthesis process of ZIF-8 has a better performance than pure ZIF-8 [19, 20]. Iron-based MOFs are a promising class of adsorbents for dye removal due to unsaturated metal active sites that facilitate strong interactions and enhance performance. For instance, Haque et al. studied the Fe-MOF-235 composite with anionic methyl orange (MO) and cationic methyl red (MR) dyes, achieving satisfactory results for both [21]. In a study [22], MOFs were investigated for removing Basic Blue 41 (BB41) dye, and the synthesized nanomaterials decolorized BB41 from wastewater. Shu-Hui et al. found that Cr-MIL-100 and Fe-MIL-100 metal hybrids adsorbed methylene blue dye with an adsorption performance of 211.8 and 1045.2 mg/g, respectively. Furthermore, MIL-100(Fe) exhibited high adsorption efficiency for malachite green (MG) pigment [23]. Ghasempour et al. studied the synthesis of Fe/MOF for dye elimination, using a variety of synthetic dyes. They

have shown an adsorption efficiency of 233 mg/g for dyes. The hydrolytically stable, highly porous Fe/MOF, with specific functional sites, shows enhanced dye elimination through improved H and π-π bonding interactions [24].

Employing bimetallic MOFs with crystalline, scaffold-like structures through a green approach could significantly enhance the treatment of anionic dyes from wastewater. This study employed a green method to synthesize a porous ZnFe/ZIF-8 (ZFZ) bimetallic composite with metal clusters and unsaturated sites, aiming to enhance performance through synergistic effects. The adsorption properties of ZFZ for Direct Red 23 (DR-23) removal were evaluated using UV-Vis spectroscopy and compared to the reference adsorbent (ZIF-8). Various adsorption kinetics mechanisms (reaction rate analysis) and adsorption isotherms (multilayer analysis) were explored.

2. Materials and methods

2.1. Materials

2-methylimidazole ($C_4H_6N_2$), zinc sulfate ($Zn(SO_4)_2{\cdot}7H_2O$), iron sulfate ($Fe(SO_4)_2{\cdot}7H_2O$), ethanol (EtOH), sodium hydroxide (NaOH), and 98% hydrochloric acid (HCL) were purchased from Merck (Germany) and used as received. DR-23 dye (a common dye in textile industries) ($C_{35}H_{25}N_7Na_2O_{10}S_2$, Mw= 813.72 g/mol) was provided by Aldrich. Figure 1 indicates the chemical structure of the DR-23 dye.

2.2. Synthesis

2.2.1. Synthesis of ZIF-8

ZIF-8 nanocrystals were synthesized by dissolving 575 mg of zinc sulfate and 1320 mg of 2-methylimidazole separately in 30 mL of deionized water under vigorous magnetic stirring. After stirring for several minutes at ambient temperature, the metal salt solution was added dropwise to the 2-methylimidazole solution. The pH of the solution was adjusted to 11.4. The yellow mixture was stirred at 45°C in an oil bath for 24 hours. The yellow precipitate was washed three times with DI water via centrifugation to remove residual ZIF-8 pore materials. The product was dried in a vacuum oven at 70°C for 12 hours.

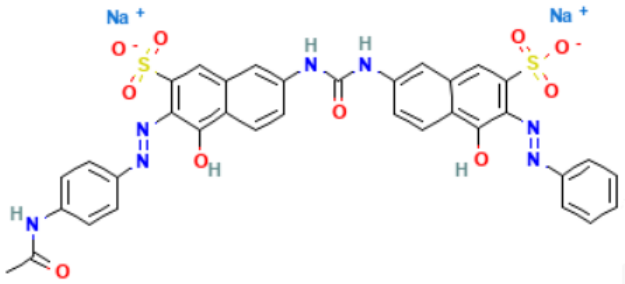

Fig. 1. Chemical structure of DR-23 dye.

2.2.2. Synthesis of ZFZ

First, a metal precursor solution was prepared by dissolving zinc sulfate (575 mg) and iron sulfate (460 mg) in deionized water (30 milliliters). Separately, a ligand solution was formed by dissolving 1.32 g of 2-methylimidazole in deionized water (30 milliliters) under vigorous magnetic stirring to obtain a fully dissolved solution (pH 11.4). The metal precursor solution was then dripped into the prepared solution under constant stirring, resulting in the immediate formation of a yellow solution. The mixture was placed in an oil bath and stirred at 45°C for 24 hours. The final solid product was isolated via centrifugation, purified through repeated washing with deionized water, and subsequently vacuum-dried at 70°C for 12 hours.

2.3. Apparatus

The chemical bonds of specimens were characterized by FTIR spectroscopy in the range of 450-4000 cm^{-1}. The phase characterization and corresponding structure of the synthesized compounds were studied with the XRD pattern (XRD device, Philips (PW1730)) under a radiation beam equipped with a copper lamp (CuKα radiation). A scanning electron microscope from TE-SCAN, model MIRA III, was uused to examine the geometric shape and imaging of the samples. An adsorption spectral study of the colored solutions was performed using a single-beam spectrophotometer of visible-ultraviolet spectroscopy (UV/Vis) in the limited wavelength area of 190-400 nm with a Biomate5 device model.

2.4. Dye Adsorption Experiment

Investigating the dyeing process of DR-23 anionic dye in a discontinuous system was prepared by adding a specific amount of synthesized

nanocomposites at a specified concentration (in a 100 ml container) at ambient temperature on a stirrer. The pH of an aliquot of the solution was adjusted to the desired value with HCl. Then, 0.006 g of the synthesized adsorbent was added to it and placed on a magnetic stirrer for a certain period at room temperature. To reach equilibrium, specimens were taken at the desired time intervals (every 15 min). The prepared sample was centrifuged to separate the pollutant. The dye concentration was measured at different times using a UV-Visible spectrophotometer. The maximum adsorption wavelength for the DR-23 appeared at 503 nm. The dye removal efficiency (R%), the adsorption capacity at time t (q_t (mg/g)), and the equilibrium adsorption of the dye (q_e (mg/g)) were calculated with Equations (1), (2), and (3).

$$R\% = \frac{(C_0 - C_t)}{C_0} * 100 \quad (1)$$

$$q_t = \frac{(C_0 - C_t)V}{m} \quad (2)$$

$$q_e = \frac{(C_0 - C_e)V}{m} \quad (3)$$

where C_o, C_t, C_e, V, and m are the initial concentration of dye (mg/l), the concentration of the dye at time t (mg/l), the equilibrium concentration of dye (mg/l), the volume of solution, and the mass of the adsorbent (g) in the solution, respectively.

3. Results and discussion

3.1. Characterization

3.1.1. FTIR

The functional groups and compositional characteristics of the ZIF-8 and ZFZ were elucidated using the FTIR technique (4000-450 cm^{-1}). Figure 2 shows the resulting spectrum of synthesized materials. The FTIR spectrum of the ZIF-8 sample aligns with previous reports [25]. The infrared spectrum of ZIF-8 (Figure 2) confirms its chemical structure.

Characteristic adsorption bands are observed at 3427 cm^{-1} (O–H stretching) and 3135 cm^{-1} (aromatic C–H stretching of the imidazole ring). Additional features include bands at 2923 cm^{-1} (aliphatic C–H stretch), 1576 cm^{-1} (C=N stretch), and in the range of 500–1000 cm^{-1} (C–H and C–C bending vibrations) [18, 19].

Critically, the spectrum of the bimetallic ZFZ composite reveals new bands at 620 cm^{-1} and 467 cm^{-1}, attributable to Fe–N and Zn–N stretching vibrations, respectively. This provides direct evidence of iron incorporation into the framework. Iron incorporation modifies the spectral profile by increasing band intensities and eliminating the C=C peak, confirming successful metal integration.

3.1.2. XRD

The phase of the ZIF-8 and ZFZ composites was established by XRD. Fig. 3 presents the XRD pattern of ZIF-8, which aligns with the literature data [25]. This figure shows that the synthesized patterns are highly similar, with differences only in peak intensity. The XRD pattern also reveals the crystal structure of the synthesized samples, with distinct crystal planes and sharp peaks indicating successful synthesis. The diagram shows that the diffraction intensity of the peaks decreases with the incorporation of iron into the ZIF-8 framework.

3.1.3. SEM

The surface morphology of the synthesized specimens was examined by SEM (Figure 4). The SEM micrographs of the ZIF-8 nanocrystals are consistent with previous research findings, confirming the reliability of the synthesis process. As evidenced by the SEM micrographs in Figure 4, the ZIF-8 particles exhibit a polyhedral structure with twelve rhombus-shaped faces, indicating successful ZIF-8 synthesis, whereas the ZFZ composite displays a modified surface texture.

The image reveals that the composition consists of spherical and uniform particles that tend to form agglomerates. This agglomeration is typical in such materials, indicating strong interparticle interactions. Notably, the surface morphology of the particles remains largely unchanged throughout the synthesis process, suggesting that the introduction of additional components, such as iron in the ZFZ composite, does not significantly alter the fundamental structural characteristics of the ZIF-8 framework [26].

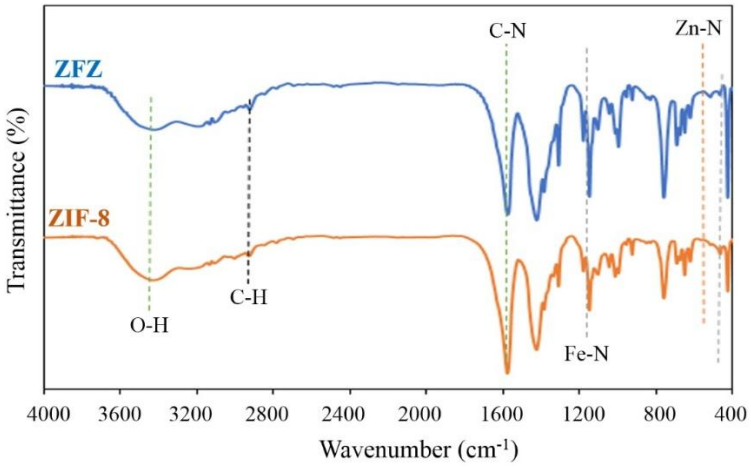

Fig. 2. FTIR spectroscopic analysis of the synthesized ZIF-8 and ZFZ composites.

This stability in morphology is crucial for maintaining the desired properties of the material, which are fundamental for applications in adsorption and catalysis. The consistent morphology also implies that the synthesis method is robust and reproducible, making it suitable for large-scale production and practical applications [3, 25].

3.2. Dye adsorption

3.2.1. Optimization of initial dye concentration

The adsorption of an anionic dye (DR-23) onto ZIF-8 and the ZFZ composite was assessed at various initial concentrations (25, 40, 55, and 70 mg/L). These experiments were performed under optimal conditions (pH 3, adsorbent dose 0.006 g) over a contact time of 0–120 minutes at laboratory temperature. Figure 5 shows the DR-23 dye removal efficiency of ZIF-8 and ZFZ with dye concentrations. According to this diagram, the removal efficiency for the ZFZ composite increased with contact time, reaching a maximum of 93% at 120 minutes, indicating its high potential for anionic dye removal. The dye removal efficiency for both adsorbents exhibited a strong inverse relationship with solution concentration. As the concentration increased from 25 to 70 mg/L, the removal efficiency for ZFZ fell from 92% to 46%, while that for ZIF-8 showed a more pronounced drop from 23% to a mere 2%.

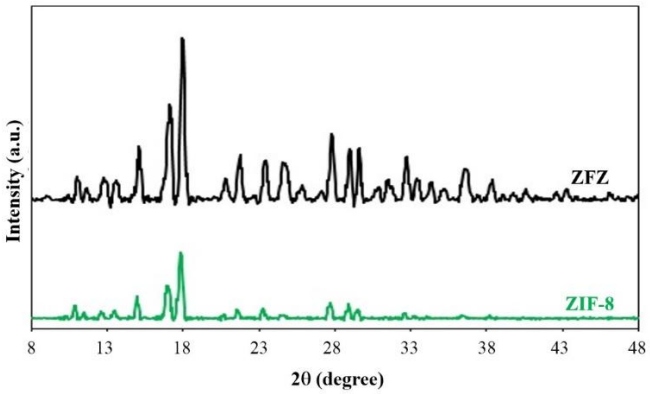

Fig. 3. XRD patterns characterizing the structure of ZIF-8 and ZFZ.

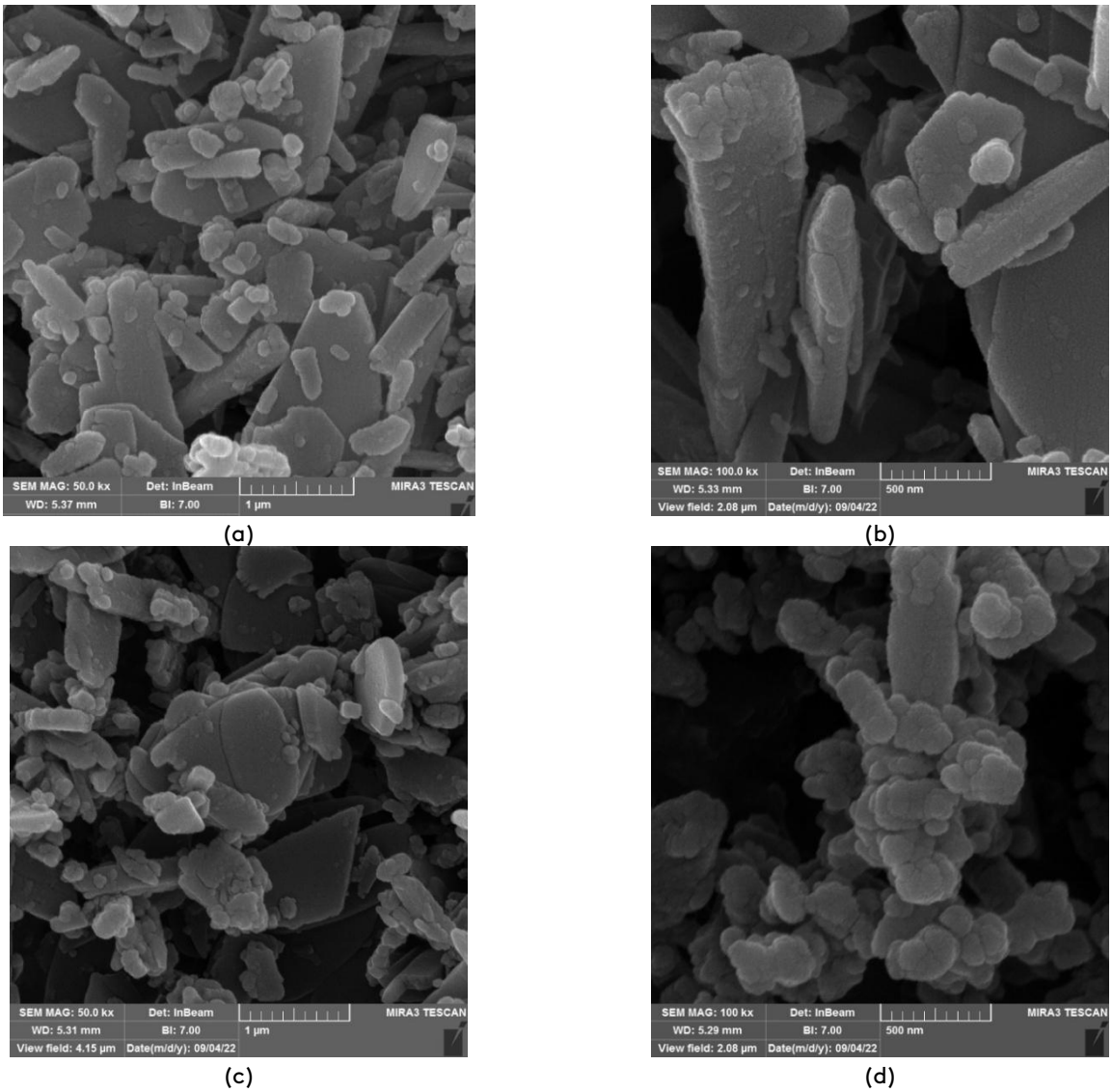

Fig. 4. SEM images of (a, b) ZIF-8 and (c, d) ZFZ composites.

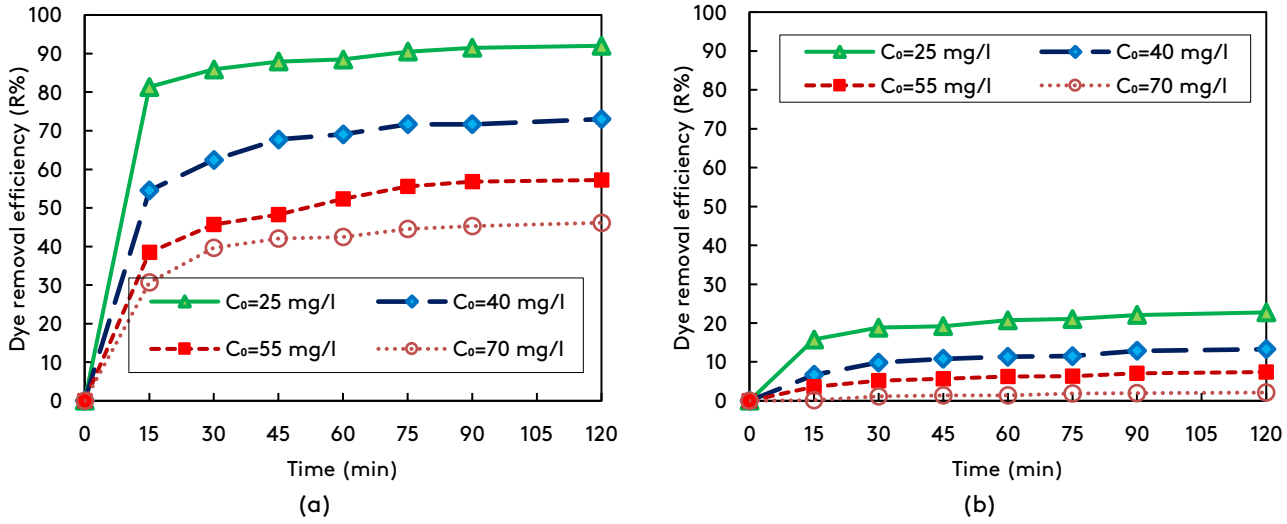

Fig. 5. Effect of initial dye concentration on removal efficiency of (a) ZFZ and (b) ZIF-8.

3.2.2. Contact time

The effect of contact time on the removal of DR-23 by ZIF-8 and ZFZ was evaluated over 120 minutes under otherwise optimal conditions (pH 3, 25 mg/L, 0.006 g adsorbent) at laboratory temperature.

Figure 6 shows the obtained results; the removal efficiency of ZFZ was 81% (88.4% Rmax) in the first 15 minutes and gradually reached 91.5% (99.4% Rmax) as the contact time increased to 90 minutes and acquired an equilibrium value of 92.1% until 120 minutes.

The temporal evolution of the system is consistent with a gradual saturation process of ZFZ available adsorption sites with anionic dye molecules.

However, it should be noted that within the adsorption process, the active and accessible sites are blocked by dye molecules and are covered entirely after a period. The adsorption rate decreases progressively as the DR-23 concentration in solution diminishes and available active sites are occupied [27, 28].

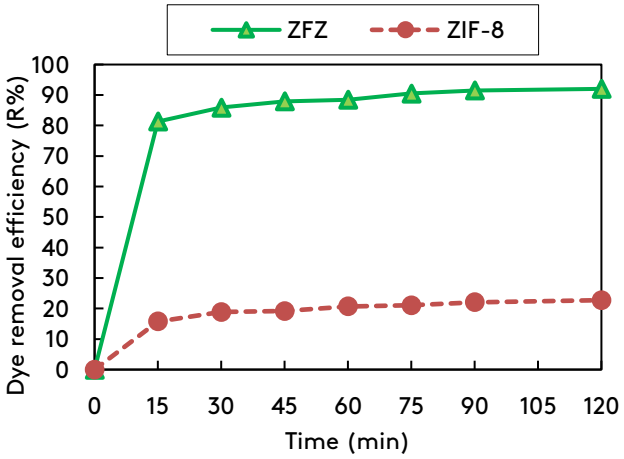

Fig. 6. The impact of time on the removal of DR-23 for (a) ZFZ and (b) ZIF-8.

3.2.3. Optimization of solution pH

The impact of solution pH on DR-23 removal by ZIF-8 and ZFZ was quantified at different pH levels (3, 4, 5, and 6) at ambient temperature. Other test variables were held constant at optimal conditions (concentration of 25 mg/L, time of 0-120 minutes, and dye dosage of 0.006 g). Figure 7 shows the effect of pH on the adsorption efficiency of DR-23 onto ZIF-8 and ZFZ. Given that the isoelectric point (pHIEP) of ZIF-8 was between 9 and 11, and considering the dye's negative charge (SO_3^-), the study focused on acidic pH levels.

As evidenced by Figure 7, the adsorption of both adsorbents for the anionic dye decreased with increasing pH, which could be described by the deprotonation of surface sites and a corresponding reduction in positive surface charge [29, 30].

Reducing the solution pH from 6 to 3 increased the efficiency of DR-23 by ZFZ from 46.7% to 92.1%. This enhancement is due to the increased protonation of the adsorbent's surface, resulting in a higher density of positive charges that electrostatically attract the anionic dye molecules.

It is important to note that the ZIF-8 may undergo minor structural degradation in acidic environments (pH < 4).

The hydrolytic instability of ZIF-8 in acidic environments is a well-documented challenge in the literature [31, 32]. In the present study, the primary adsorbent investigated was ZnFe/ZIF-8, in which the incorporation of Fe species is expected to enhance framework robustness compared to pristine ZIF-8, as reported in previous studies [33]. While post-adsorption XRD or FTIR analysis was not performed in this study to quantify this effect, the significant enhancement in dye adsorption capacity observed for the ZnFe/ZIF-8 composite compared to pristine ZIF-8 under identical acidic conditions suggests a consequential difference in material behavior.

The superior performance of the composite could be attributed not only to its modified surface properties but also to potentially improved acid stability imparted by iron doping, a hypothesis that warrants dedicated future investigation. However, the structural stability of ZnFe/ZIF-8 under these conditions cannot be definitively confirmed within the scope of this work. Therefore, for any practical application, the long-term stability of the adsorbent in acidic effluent streams would be a crucial factor for further study.

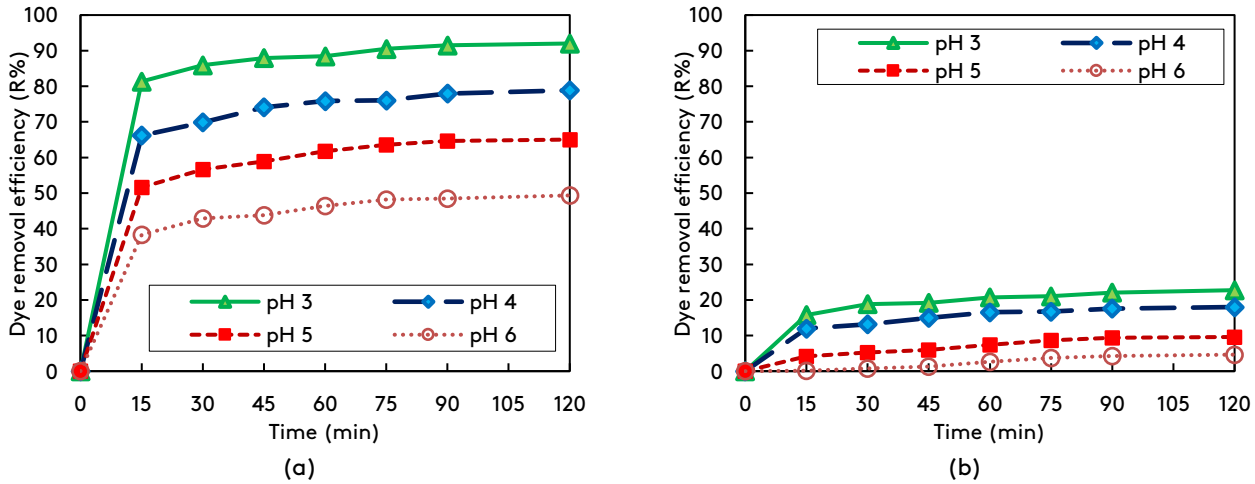

Fig. 7. Impact of pH on DR-23 removal of (a) ZFZ, and (b) ZIF-8.

3.2.4. Optimization of adsorbent dosage

The impact of adsorbent mass on the removal efficiency of DR-23 was examined using ZIF-8 and ZFZ at varying masses (0.003, 0.004, 0.005, and 0.006 g) at room temperature. Other test variables were maintained at optimal values, including pH (3), concentration (25 mg/L), and a time range of 0-120 minutes. The results are presented in Figure 8. The efficiency of both adsorbents increased rapidly with dosage, reaching equilibrium after 120 minutes. The ZFZ nanocomposite consistently demonstrated superior performance, achieving a 92% removal rate compared to ZIF-8. This significant enhancement in adsorption capacity is attributed to the iron doping within the ZIF-8 framework, which improves the material's adsorptive surface properties and increases the abundance of active sites available for dye interaction [34-36]. Based on these results, an optimal adsorbent dosage of 6 mg was selected for subsequent experiments.

3.2.5. Adsorption Isotherms

An adsorption isotherm quantifies the equilibrium uptake of an adsorbate by a solid surface. Equilibrium appears when the adsorption rate of adsorbed molecules on the absorbent surface is equal to their desorption rate.

The isotherms of Freundlich, Langmuir, and Temkin were discussed to better understand and analyze the obtained results. The isotherm variables are presented in Table 1. The equilibrium adsorption data for both composites were evaluated using Langmuir, Freundlich, and Temkin models (Figure 9). The study investigated the effects of ZIF-8 and ZFZ adsorbents on the removal of DR-23 dye. Different amounts of the adsorbents (0.003, 0.004, 0.005, and 0.006 grams) were added at an optimal dye concentration of 25 mg/L, with a contact time of 120 minutes, all at an acidic pH of 3. Table 1 shows the obtained results. The Langmuir model has R^2 values of 0.99 for ZFZ and 0.94 for ZIF-8. The close alignment with the Langmuir model indicates a homogeneous surface with monolayer coverage, consistent with a physisorption mechanism [37-39].

Langmuir's linear equation is explicated as Equation (4).

$$\frac{C_e}{q_e} = \frac{1}{K_l \cdot q_l} + \frac{C_e}{q_l} \quad (4)$$

where q_e (mg/g) is the equilibrium adsorption capacity, C_e (mg/L) is the equilibrium liquid-phase concentration, q_{max} (mg/g) is the maximum monolayer adsorption capacity, and K_L (L/mg) is the Langmuir constant. The Freundlich model can be used to determine whether the desired purity level can be achieved with a given adsorbent [27, 40]. Freundlich's linear equation is expressed as Equation (5):

$$\log q_e = \log K_f + \frac{1}{n} \log C_e \quad (5)$$

where the factors n and K_f (L/g) are respectively related to the Freundlich constant (expressing capacity) and the adsorption intensity.

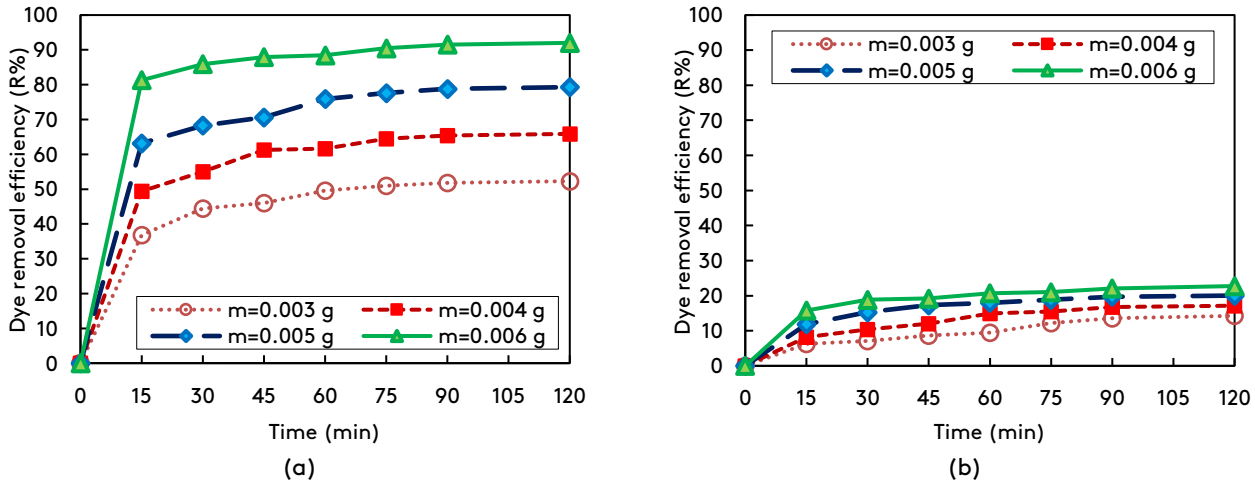

Fig. 8. Impact of adsorbent dosage on DR-23 removal with (a) ZFZ; (b) ZIF-8.

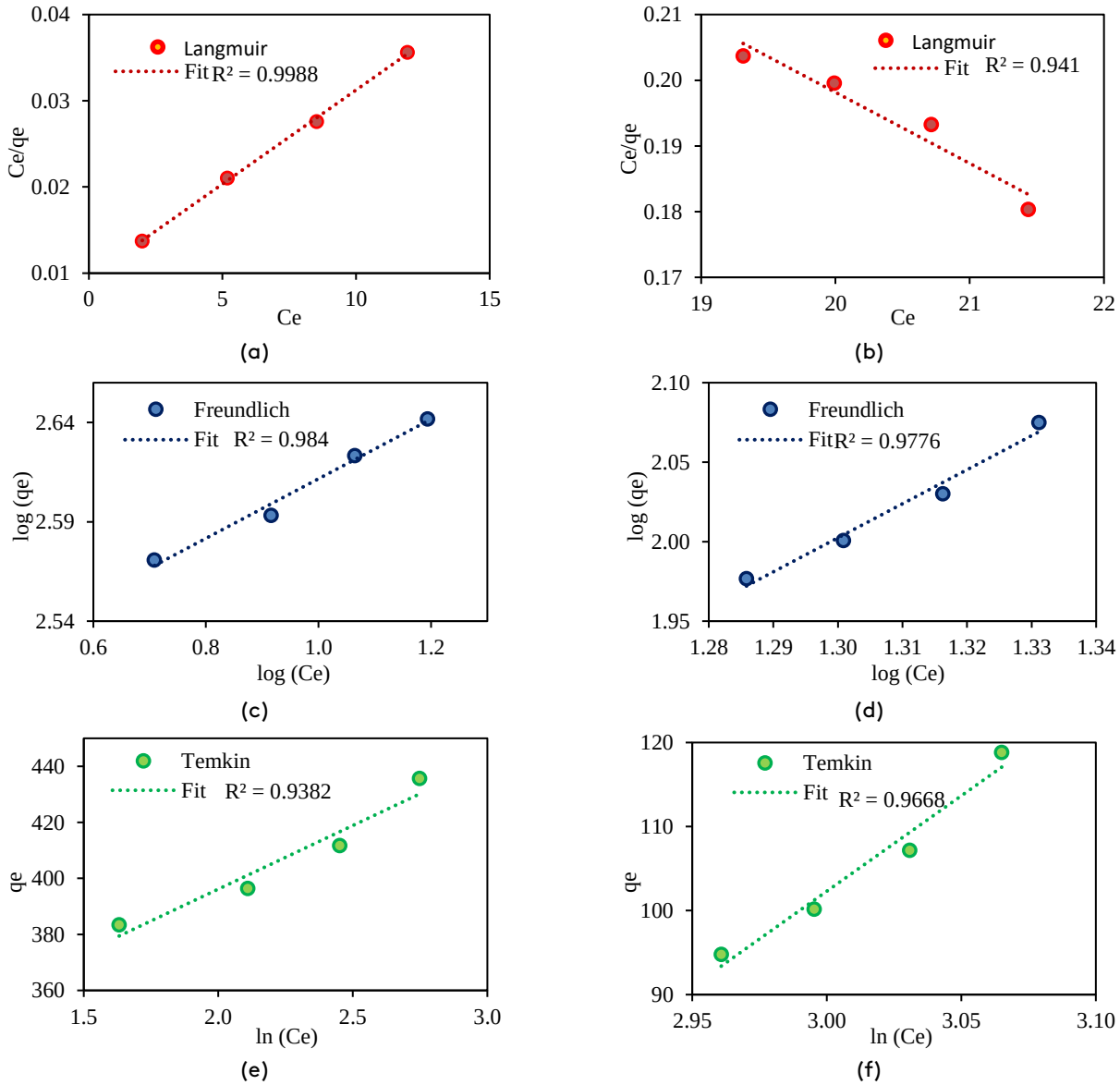

Fig. 9. The isotherms of Langmuir (a) ZFZ; (b) ZIF-8 and Freundlich (c) ZFZ; (d) ZIF-8 and Temkin (e) ZFZ; (f) ZIF-8.

Table 1. Fitted isotherm variables for DR-23 removal using ZFZ and ZIF-8.

Model name	Parameters	ZFZ	ZIF-8
Langmuir	q_L (mg/g)	454.54	92.59
	K_L (L/mg)	0.23	0.02
	R^2	0.99	0.94
Freundlich	K_F ((mg/g)/(mg/L)$^{1/n}$)	289.53	06.03
	n	6.67	0.46
	R^2	0.98	0.97
Temkin	K_T (L/g)	830.96	12.80
	B_T (J/mol)	45.41	227.17
	R^2	0.93	0.96

Temkin's model assumes that by neglecting very low and high concentrations of dyes, the isosteric heat of adsorption exhibits a linear decline as a function of surface coating, a phenomenon resulting from repulsive interactions between adsorbed molecules [38, 41]. Temkin's linear equation is expressed as relation (6):

$$q_e = B_T \ln K_T + B_T \ln C_e \quad (6)$$

In this equation, the coefficients (constants of the Temkin model) K_T (L/g) and B_T (J/mol) show the heat of adsorption.

3.2.6. Adsorption kinetic models

Kinetic modeling of the adsorption process clarifies the underlying mechanisms and interfacial dynamics. This kinetic behavior is governed by the physicochemical characteristics of the adsorbent [41, 42]. The adsorption kinetics of DR-23 on the synthesized materials were investigated using adsorbent masses of 0.003–0.006 g at optimal conditions (concentration of 25 mg/L, pH of 3, and a 120-minute contact time). The resulting kinetic data were fitted to the pseudo-first-order (PFO), pseudo-second-order (PSO), and Intraparticle Diffusion (IPD) models. The PFO kinetic model assumes that adsorption occurs due to the difference in concentration between the adsorbing and calcined surfaces, which is linked to the external mass transfer coefficient [43, 44]. The PSO kinetic model assumes that chemical adsorption controls the process [36, 45]. Penetration within the particles (IPD kinetic model) indicates multi-step adsorption, including the migration of solutes from the aqueous phase to the solid sorbent surface and their subsequent diffusion into the internal pores of the adsorbent [46-48]. The linearized relations of the PFO, PSO, and IPD models are defined as Equations (7), (8), and (9), respectively.

$$log(q_e - q_t) = log\, q_e - \frac{k_1 t}{2.303} \quad (7)$$

$$\frac{t}{q_t} = \frac{1}{k_2 {q_e}^2} + \frac{t}{q_e} \quad (8)$$

$$q_t = k_p t^{1/2} + I \quad (9)$$

where q_e , q_t , k_1 , k_2 , k_p , I , t are the adsorption capacity at equilibrium (mg/g), the adsorption capacity at time t (mg/g), the pseudo-first order adsorption rate constant (min^{-1}), the pseudo-second order adsorption rate constant (g/mg min), the constant of the intraparticle diffusion rate (mg/g $min^{0.5}$), the constant of the intraparticle diffusion, and time (min), respectively. Figure 10 shows the linearized PFO (a, b), PSO (c, d), and IPD (e, f) kinetic models (Equations 7-9) for DR-23 adsorption on ZFZ (a, c, e) and ZIF-8 (b, d, f). To compare the kinetic models and better analyze the results, their parameters were estimated and are presented in Table 2. The PSO model provided an excellent fit for the DR-23 adsorption data across all doses of both ZFZ and ZIF-8, with high regression coefficients of 0.99 for ZFZ and between 0.98 and 0.99 for ZIF-8. The equilibrium adsorption capacity (q_e) estimated by the PSO model closely matches the experimentally determined value. Therefore, the controlling mechanism for the DR-23 dye adsorption on ZFZ composites and ZIF-8 was ion exchange by electrostatic interactions, which had a primary role. The IPD kinetic model demonstrated a poor fit to the observed data (low R^2 values). This implies that diffusion within the particles was not the rate-limiting step, and adsorption likely occurred mainly on the surface. The adsorption performance of the ZnFe/ZIF-8 (ZFZ) composite significantly exceeded that of pristine ZIF-8. Under

optimal conditions (adsorbent dosage = 0.06 g), the equilibrium adsorption capacity (q_e) of ZFZ for DR-23 reached 383.41 mg/g, which is approximately four times greater than the capacity of ZIF-8 (94.79 mg/g). A further increase in q_e to 435.76 mg/g was observed at a lower dosage of 0.003 g (Table 2), highlighting the material's high efficiency even with minimal adsorbent loading. As summarized in Table 3, the q_e of ZFZ (383.41 mg/g at pH 3) is highly competitive with state-of-the-art adsorbents, including engineered polymers, composite materials, and various metal-organic frameworks (MOFs) reported for DR-23 dye removal.

This comparative analysis underscores that the iron-doped ZIF-8 composite developed via a green aqueous synthesis route is not only effective but also a promising sustainable alternative for water remediation applications.

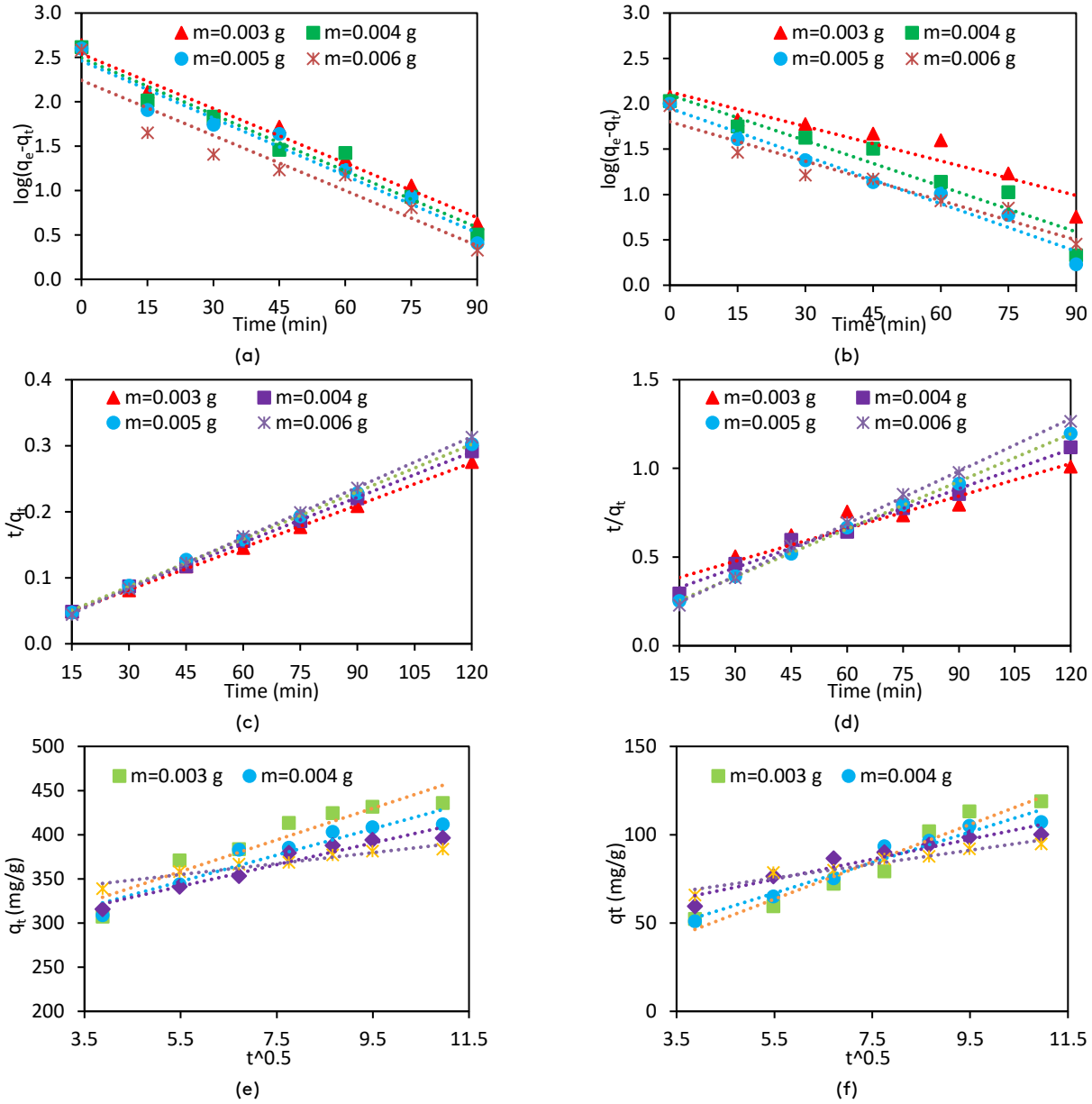

Fig. 10. The observed data fit with PFO: (a) ZFZ & (b) ZIF-8 and; PSO: (c) ZFZ & (d) ZIF-8, and IPD: (e) ZFZ & (f) ZIF-8 for removal of DR-23.

Table 2. The kinetic models' parameters for DR-23 removal by ZFZ & ZIF-8.

Adsorbent	dose (g)	(q_e) Exp. (mg/g)	Pseudo-first-order (PFO)			Pseudo-second-order (PSO)			Intraparticle diffusion (IPD)		
			(q_e) Cal. (mg/g)	k_1	R^2	(q_e) Cal. (mg/g)	k_1	R^2	k_p	I	R^2
ZIF-8	0.003	118.84	135.53	0.055	0.87	163.93	0.0001	0.98	10.56	05.43	0.94
	0.004	107.17	125.22	0.007	0.93	135.13	0.0002	0.98	08.64	19.42	0.95
	0.005	100.16	89.14	0.007	0.96	102.41	0.0007	0.99	05.67	43.54	0.92
	0.006	94.79	63.41	0.006	0.93	101.01	0.0010	0.99	03.94	53.78	0.94
ZFZ	0.003	435.76	345.78	0.008	0.97	476.19	0.0002	0.99	17.91	259.75	0.89
	0.004	411.71	311.53	0.009	0.96	434.78	0.0003	0.99	14.92	264.95	0.89
	0.005	396.43	289.41	0.009	0.95	416.66	0.0003	0.99	12.25	274.07	0.93
	0.006	383.41	174.52	0.008	0.91	384.61	0.0009	0.99	06.19	30.82	0.92

Table 3. Comparison of different adsorbents for DR-23 dye adsorption under optimal pH conditions.

Adsorbent	Optimal pH	Maximum Adsorption Capacity (mg/g)	Ref.
Cu-BTC–NH_2 (modified)	2.1	2500	[49]
Al/nanoclay–MOF composite	2	2500	[50]
NH2-MIL-88B	2.1	2500	[51]
ZIF-8@APTMS	2.2	2150	[52]
PAN/PAMAM	2.1	2000	[53]
Fe3O4@SA-Fe	2	1429	[54]
Functionalized PAN nanofibers (FPAN) reaction for diethylamine (FPAN1)	2.1	185.73	[55]
Functionalized PAN nanofibers (FPAN) reaction for diethylenetriamine (FPAN2)	2.1	1194.66	[55]
Functionalized PAN nanofibers (FPAN) reaction for triethylenetetramine (FPAN3)	2.1	4,511.27	[55]
TM-PAN	3.5	1250	[56]
DETA-PAN/PVDF	2	685.63	[57]
Fe/Cr-codoped ZnO NPs	7	642.25	[58]
PVA/CS/DETA/EDA	2.1	526.31	[59]
AS-CTAB	2	454.9	[60]
Zn-MOF@polymer hybrid	5	410	[61]
modified nanofiber	3	370	[62]
montmorillonite nanoclay	3	166.6	[63]
Powdered Tourmaline	3	153	[64]
CS-g-PNEANI	2	112	[65]
CAC/MIL-53(Fe)	3	100	[26]
MIL-88B	2.1	100	[51]
Cu-BTC (C-BTC)	2.1	89.2857	[49]
rGO/CTAB	11	79	[66]
Cationized sawdust	5.5	65.8	[67]
Cell/PANI	2	56	[68]
Commercial Activated Carbon (CAC)	3	50	[26]
Zno	7	28.48	[58]
ZIF-8	3	94.79	This study
ZnFe/ZIF-8 (ZFZ)	3	383.41	This study

4. Conclusion

Iron metal doping successfully enhanced the performance of ZIF-8, creating the ZFZ composite through a green synthesis method that maximizes synergistic effects. The produced ZFZ composite and ZIF-8 were characterized using FTIR, XRD, and SEM. Analysis of the observed data revealed that iron metal doping on ZIF-8 improves the physical properties (mechanical, crystallinity, etc.), as well as the adsorption properties of the adsorbent. While BET data would be valuable for full textural characterization (porosity and surface area), the conclusions of this study regarding adsorption efficacy are grounded in functional performance tests. The following key parameters influence the dye adsorption: dye concentration, solution pH, adsorbent mass, and contact time. The highest adsorption capacity of the synthesized ZFZ composite was achieved at a solution pH of 3, concentration of 25 mg/L, adsorbent dosage of 0.06 g, and a contact time of 120 minutes. These values were considered the optimal conditions of this study for DR-23 dye removal from wastewater. The ZFZ composite demonstrated a significantly higher DR-23 removal efficiency (92%) compared to pristine ZIF-8 (22.8%), representing a four-fold enhancement. The observed adsorption data for ZFZ were well fit by the Langmuir model ($R^2 > 0.99$), indicating a homogeneous monolayer adsorption. Moreover, the measurement adsorption kinetics data for both ZFZ and ZIF-8 complied with the PSO model (R^2 of 0.99) for each composite. Overall, the findings suggest that ZFZ is a highly efficient and environmentally benign material, positioning it as a compelling candidate for integration into water treatment technologies aimed at removing anionic dyes.

Author's contribution

All authors contributed equally to the conception, design, data analysis, drafting, and revision of this manuscript. All authors read and approved the final version of the manuscript.

Conflict of interest

No potential conflict of interest was reported by the authors.

Data availability

Not applicable.

Funding

Self-funded.

References

[1] Hussain, T. S., & Al-Fatlawi, A. H. (2020). Remove chemical contaminants from potable water by household water treatment system. *Civil Engineering Journal, 6*(8), 1534-1546. https://doi.org/10.28991/cej-2020-03091565

[2] Reinsch, H. (2016). "Green" synthesis of metal-organic frameworks. *European Journal of Inorganic Chemistry, 2016*(27), 4290-4299. https://doi.org/10.1002/ejic.201600286

[3] Shahsavari, M., Mohammadzadeh Jahani, P., Sheikhshoaie, I., Tajik, S., Aghaei Afshar, A., Askari, M. B., Salarizadeh, P., Di Bartolomeo, A., & Beitollahi, H. (2022). Green synthesis of zeolitic imidazolate frameworks: a review of their characterization and industrial and medical applications. *Materials, 15*(2), 447. https://doi.org/10.3390/ma15020447

[4] Omar, M. E. D. M., Moussa, A. M. A., & Hinkelmann, R. (2021). Impacts of climate change on water quantity, water salinity, food security, and socioeconomy in Egypt. *Water Science and Engineering, 14*(1), 17-27. https://doi.org/10.1016/j.wse.2020.08.001

[5] Mirkhalafi, S., Mohammadnezhad, B., Mousazadehgavan, M., Kiehbadroudinezhad, M., Altaee, A., Hosseinzadeh-Bandbafha, H., & Hashim, K. (2025). Technical and Environmental Sustainability of Pharmaceutical Wastewater Treatment Using Ce-NaY Zeolite-Modified Polyethersulfone (PES) Membranes: A Life Cycle Assessment Approach. *ACS ES&T Water, 5*(7), 3818-3830. https://doi.org/10.1021/acsestwater.5c00162

[6] Mirkhalafi, S., Mohammadnezhad, B., Mousazadehgavan, M., Altaee, A., Kiehbadroudinezhad, M., Hosseinzadeh-Bandbafha, H., Hashim, K., & Mohammadi, M. (2025). Ni-NaY Zeolite-Modified Polyethersulfone Membranes for Sustainable Water Treatment: Enhanced Flux, Contaminant Rejection, and Life Cycle

Assessment. *Microporous and Mesoporous Materials*, 113958. https://doi.org/10.1016/j.micromeso.2025.113958

[7] Iman, K., Shahid, M., Khan, M. S., Ahmad, M., & Sama, F. (2019). Topology, magnetism and dye adsorption properties of metal organic frameworks (MOFs) synthesized from bench chemicals. *CrystEngComm, 21*(35), 5299-5309. https://doi.org/10.1039/C9CE01041F

[8] Phuengphai, P., Singjanusong, T., Kheangkhun, N., & Wattanakornsiri, A. (2021). Removal of copper (II) from aqueous solution using chemically modified fruit peels as efficient low-cost biosorbents. *Water Science and Engineering, 14*(4), 286-294. https://doi.org/10.1016/j.wse.2021.08.003

[9] Xu, Q., Sun, D., Qi, Y., & Duan, L. (2019). Efficient Removal of Anionic Organic Dyes from Aqueous Solution with Cu-Organic Frameworks. *Chemical Engineering & Technology, 42*(5), 1070-1077. https://doi.org/10.1002/ceat.201800398

[10] Azizi, A., Moniri, E., Hassani, A. H., & Ahmad Panahi, H. (2020). Reusability, optimization, and adsorption studies of modified graphene oxide in the removal of Direct Red 81 using response surface methodology. *Advances in Environmental Technology, 6*(4), 175-185. https://doi.org/10.22104/aet.2021.4347.1239

[11] Askari, N., Farhadian, M., & Razmjou, A. (2015). Decolorization of ionic dyes from synthesized textile wastewater by nanofiltration using response surface methodology. *Advances in Environmental Technology, 1*(2), 85-92. https://doi.org/10.22104/aet.2015.192

[12] Venu, B., Shirisha, V., Vishali, B., Naresh, G., Kishore, R., Sreedhar, I., & Venugopal, A. (2020). A Cu-BTC metal–organic framework (MOF) as an efficient heterogeneous catalyst for the aerobic oxidative synthesis of imines from primary amines under solvent free conditions. *New Journal of Chemistry, 44*(15), 5972-5979. https://doi.org/10.1039/C9NJ05997K

[13] Aarti, A., Bhadauria, S., Nanoti, A., Dasgupta, S., Divekar, S., Gupta, P., & Chauhan, R. (2016). [Cu3 (BTC) 2]-polyethyleneimine: an efficient MOF composite for effective CO2separation. *Rsc Advances, 6*(95), 93003-93009. https://doi.org/10.1039/C6RA10465G

[14] Schejn, A., Aboulaich, A., Balan, L., Falk, V., Lalevée, J., Medjahdi, G., Aranda, L., Mozet, K., & Schneider, R. (2015). Cu 2+-doped zeolitic imidazolate frameworks (ZIF-8): efficient and stable catalysts for cycloadditions and condensation reactions. *Catalysis Science & Technology, 5*(3), 1829-1839. https://doi.org/10.1039/C4CY01505C

[15] Huang, A., Liu, Q., Wang, N., Zhu, Y., & Caro, J. r. (2014). Bicontinuous zeolitic imidazolate framework ZIF-8@ GO membrane with enhanced hydrogen selectivity. *Journal of the American Chemical Society, 136*(42), 14686-14689. https://doi.org/10.1021/ja5083602

[16] Soleimani, R., Mohammadnezhad, B., & Hosseini, S. A. (2025). Green Synthesis of ZnNi/ZIF-8 Composites for Efficient Anionic Dye Removal: A Sustainable Approach to Wastewater Treatment. *Current Research in Green and Sustainable Chemistry*, 100487. https://doi.org/10.1016/j.crgsc.2025.100487

[17] Soleimani, R., Mohammadnezhad, B., Hosseini, S. A., & Khaleghi Moghaddam, M. (2025). Dyes Adsorption from Wastewater Using Metal-Organic Frameworks: Operational Parameters, Kinetics, and Isotherms. *Journal of Studies in Color World*. https://doi.org/10.30509/jscw.2025.167614.1251

[18] Jamil, N., Alias, N. H., Shahruddin, M. Z., & Othman, N. H. (2019). A green in situ synthesis of hybrid graphene-based zeolitic imidazolate framework-8 nanofillers using recycling mother liquor. *Key Engineering Materials, 797*, 48-54. https://doi.org/10.4028/www.scientific.net/KEM.797.48

[19] Tran, B. L., Chin, H.-Y., Chang, B. K., & Chiang, A. S. (2019). Dye adsorption in ZIF-8: The importance of external surface area. *Microporous and Mesoporous Materials, 277*, 149-153. https://doi.org/10.1016/j.micromeso.2018.10.027

[20] Liu, J., He, J., Wang, L., Li, R., Chen, P., Rao, X., Deng, L., Rong, L., & Lei, J. (2016). NiO-PTA supported on ZIF-8 as a highly

effective catalyst for hydrocracking of Jatropha oil. *Scientific reports, 6*(1), 23667. https://doi.org/10.1038/srep23667

[21] Haque, E., Jun, J. W., & Jhung, S. H. (2011). Adsorptive removal of methyl orange and methylene blue from aqueous solution with a metal-organic framework material, iron terephthalate (MOF-235). *Journal of Hazardous materials, 185*(1), 507-511. https://doi.org/10.1016/j.jhazmat.2010.09.035

[22] Mahmoodi, N. M., Abdi, J., Oveisi, M., Asli, M. A., & Vossoughi, M. (2018). Metal-organic framework (MIL-100 (Fe)): Synthesis, detailed photocatalytic dye degradation ability in colored textile wastewater and recycling. *Materials Research Bulletin, 100*, 357-366. https://doi.org/10.1016/j.materresbull.2017.12.033

[23] Shu, H., & Xiu, P. (2012). Metal-organic framework MIL-100 (Fe) for the adsorption of malachite green from aqueous solution. *J. Mater. Chem, 22*, 7449-7455. https://doi.org/10.1039/C2JM16513A

[24] Ghasempour, H., Zarekarizi, F., & Morsali, A. (2022). Acyl amide-functionalized and water-stable iron-based MOF for rapid and selective dye removal. *CrystEngComm, 24*(22), 4074-4084. https://doi.org/10.1039/D2CE00369D

[25] Ye, G., Zhao, K., He, Z., Huang, R., Liu, Y., & Liu, S. (2018). Fe-N x sites enriched carbon micropolyhedrons derived from Fe-doped zeolitic imidazolate frameworks with reinforced Fe-N coordination for efficient oxygen reduction reaction. *ACS Sustainable Chemistry & Engineering, 6*(11), 15624-15633. https://doi.org/10.1021/acssuschemeng.8b04105

[26] Soroush, S., Mahmoodi, N. M., Mohammadnezhad, B., & Karimi, A. (2022). Activated carbon (AC)-metal-organic framework (MOF) composite: Synthesis, characterization and dye removal. *Korean Journal of Chemical Engineering, 39*(9), 2394-2404. https://doi.org/10.1007/s11814-022-1100-9

[27] Jawad, A. H., Abdulhameed, A. S., Reghioua, A., & Yaseen, Z. M. (2020). Zwitterion composite chitosan-epichlorohydrin/zeolite for adsorption of methylene blue and reactive red 120 dyes. *International Journal of Biological Macromolecules, 163*, 756-765. https://doi.org/10.1016/j.ijbiomac.2020.07.014

[28] Zha, Q., Sang, X., Liu, D., Wang, D., Shi, G., & Ni, C. (2019). Modification of hydrophilic amine-functionalized metal-organic frameworks to hydrophobic for dye adsorption. *Journal of Solid State Chemistry, 275*, 23-29. https://doi.org/10.1016/j.jssc.2019.04.001

[29] Mohammadi, L., Bazrafshan, E., Noroozifar, M., Ansari-Moghaddam, A., Barahuie, F., & Balarak, D. (2017). Adsorptive removal of benzene and toluene from aqueous environments by cupric oxide nanoparticles: kinetics and isotherm studies. *Journal of Chemistry, 2017*. https://doi.org/10.1155/2017/2069519

[30] Al-Degs, Y. S. (2008). El-Barghouthi., MI El-Sheikh, AH & Walker, GM (2008) Effect of solution pH, ionic strength, and temperature on adsorption behaviour of reactive dyes on activated carbon. *Dyes and pigments, 77*, 16-23. https://doi.org/10.1016/j.dyepig.2007.03.001

[31] Zhang, H., James, J., Zhao, M., Yao, Y., Zhang, Y., Zhang, B., & Lin, Y. (2017). Improving hydrostability of ZIF-8 membranes via surface ligand exchange. *Journal of Membrane Science, 532*, 1-8. https://doi.org/10.1016/j.memsci.2017.01.065

[32] Pang, S. H., Han, C., Sholl, D. S., Jones, C. W., & Lively, R. P. (2016). Facet-specific stability of ZIF-8 in the presence of acid gases dissolved in aqueous solutions. *Chemistry of Materials, 28*(19), 6960-6967. https://doi.org/10.1021/acs.chemmater.6b02643

[33] Anbari, A. P., Delcheh, S. R., Kashif, M., Ranjbari, A., Karbalaei Akbari, M., Zhuiykov, S., Heynderickx, P. M., & Verpoort, F. (2025). Engineering Fe-Modified Zeolitic Imidazolate Frameworks (Fe-ZIF-8 and Fe-ZIF-67) via In Situ Thermal Synthesis for Enhanced Adsorption of Malachite Green from Aqueous Solutions: A Comprehensive Study of Isotherms, Kinetics, and Thermodynamics. *Nanomaterials, 15*(14), 1097. https://doi.org/10.3390/nano15141097

[34] Jaafari, J., Barzanouni, H., Mazloomi, S., Farahani, N. A. A., Sharafi, K., Soleimani, P., &

Haghighat, G. A. (2020). Effective adsorptive removal of reactive dyes by magnetic chitosan nanoparticles: kinetic, isothermal studies and response surface methodology. *International Journal of Biological Macromolecules, 164*, 344-355. https://doi.org/10.1016/j.ijbiomac.2020.07.042

[35] Al Sharabati, M., & Sabouni, R. (2020). Selective removal of dual dyes from aqueous solutions using a metal organic framework (MIL-53 (Al)). *Polyhedron, 190*, 114762. https://doi.org/10.1016/j.poly.2020.114762

[36] Natarajan, R., Banerjee, K., Kumar, P. S., Somanna, T., Tannani, D., Arvind, V., Raj, R. I., Vo, D.-V. N., Saikia, K., & Vaidyanathan, V. K. (2021). Performance study on adsorptive removal of acetaminophen from wastewater using silica microspheres: Kinetic and isotherm studies. *Chemosphere, 272*, 129896. https://doi.org/10.1016/j.chemosphere.2021.129896

[37] Choy, K. K., Porter, J. F., & McKay, G. (2000). Langmuir isotherm models applied to the multicomponent sorption of acid dyes from effluent onto activated carbon. *Journal of Chemical & Engineering Data, 45*(4), 575-584. https://doi.org/10.1021/je9902894

[38] Langmuir, D. A. (2012). Dubinin-Radushkevich Isotherms Studies of Equilibrium Sorption of Zn2+ Unto Phosphoric Acid Modified Rice Husk/AO Dada, AP Olalekan, AM Olatunya. *Journal of Applied Chemistry, 3*, 38-45. http://dx.doi.org/10.9790/5736-0313845

[39] Li, L., Yang, L., Zou, R., Lan, J., Shang, J., Dou, B., Liu, H., & Lin, S. (2021). Facile and scalable preparation of ZIF-67 decorated cotton fibers as recoverable and efficient adsorbents for removal of malachite green. *Journal of Leather Science and Engineering, 3*, 1-15. https://doi.org/10.1186/s42825-021-00069-w

[40] Vadivelan, V., & Kumar, K. V. (2005). Equilibrium, kinetics, mechanism, and process design for the sorption of methylene blue onto rice husk. *Journal of colloid and interface science, 286*(1), 90-100. https://doi.org/10.1016/j.jcis.2005.01.007

[41] Guo, H., Lin, F., Chen, J., Li, F., & Weng, W. (2015). Metal–organic framework MIL-125 (Ti) for efficient adsorptive removal of Rhodamine B from aqueous solution. *Applied Organometallic Chemistry, 29*(1), 12-19. https://doi.org/10.1002/aoc.3237

[42] Thombare, N., Mishra, S., Shinde, R., Siddiqui, M., & Jha, U. (2021). Guar gum based hydrogel as controlled micronutrient delivery system: Mechanism and kinetics of boron release for agricultural applications. *Biopolymers, 112*(3), e23418. https://doi.org/10.1002/bip.23418

[43] Ansari-Asl, Z., Darvish Pour-Mogahi, S., & Darabpour, E. (2023). Zeolitic imidazolate frameworks/polyacrylonitile composites for oil sorption and antibacterial applications. *Applied Nanoscience, 13*(1), 369-381. https://doi.org/10.1007/s13204-021-01745-3

[44] Firouzjaei, M. D., Afkhami, F. A., Esfahani, M. R., Turner, C. H., & Nejati, S. (2020). Experimental and molecular dynamics study on dye removal from water by a graphene oxide-copper-metal organic framework nanocomposite. *Journal of Water Process Engineering, 34*, 101180. https://doi.org/10.1016/j.jwpe.2020.101180

[45] Thanh, M. T., Thien, T. V., Du, P. D., Hung, N. P., & Khieu, D. Q. (2018). Iron doped zeolitic imidazolate framework (Fe-ZIF-8): synthesis and photocatalytic degradation of RDB dye in Fe-ZIF-8. *Journal of Porous Materials, 25*, 857-869. https://doi.org/10.1007/s10934-017-0498-7

[46] Rohart, A., Moulin, G., & Michon, C. (2014). Interplay between phase separation and gel formation in stirred acid milk/guar gum gels: Effect of acidification rate. *Biopolymers, 101*(9), 966-974. https://doi.org/10.1002/bip.22484

[47] Zhao, C., Liu, Y., Meng, M., Li, Z., Wang, H., Liu, W., & Yang, X. (2022). Research on Adsorption and Desorption Performance of Gas-Phase Naphthalene on Hydrophobic Modified FDU-15. *Processes, 10*(3), 574. https://doi.org/10.3390/pr10030574

[48] Aksu, Z. (2005). Application of biosorption for the removal of organic pollutants: a review. *Process biochemistry, 40*(3-4), 997-1026. https://doi.org/10.1016/j.procbio.2004.04.008

[49] Amirahmadi, S., Moradi, O., & Arab-Salmanabadi, S. (2024). The adsorption of direct red 23 as a toxic pollutant in aqueous solution by using surface modified metal-organic framework containing tricarboxylic acid benzene ligand. *Desalination and Water Treatment, 317*, 100132. https://doi.org/10.1016/j.dwt.2024.100132

[50] Pormazar, S. M., & Dalvand, A. (2020). Adsorption of Direct Red 23 dye from aqueous solution by means of modified montmorillonite nanoclay as a superadsorbent: mechanism, kinetic and isotherm studies. *Korean Journal of Chemical Engineering, 37*(12), 2192-2201. https://doi.org/10.1007/s11814-020-0629-8

[51] Moradi, O., & Sharabaf, I. D. (2022). Separation of organic contaminant (dye) using the modified porous metal-organic framework (MIL). *Environmental Research, 214*, 114006. https://doi.org/10.1016/j.envres.2022.114006

[52] Bagheri, A., Hoseinzadeh, H., Hayati, B., Mahmoodi, N. M., & Mehraeen, E. (2021). Post-synthetic functionalization of the metal-organic framework: Clean synthesis, pollutant removal, and antibacterial activity. *Journal of Environmental Chemical Engineering, 9*(1), 104590. https://doi.org/10.1016/j.jece.2020.104590

[53] Almasian, A., Mahmoodi, N. M., & Olya, M. E. (2015). Tectomer grafted nanofiber: Synthesis, characterization and dye removal ability from multicomponent system. *Journal of Industrial and Engineering Chemistry, 32*, 85-98. https://doi.org/10.1016/j.jiec.2015.08.002

[54] Lv, T., & Li, B. (2021). Preparation of novel magnetic sodium alginate-ferric (III) gel beads and their super-efficient removal of direct dyes from water. *Journal of Polymers and the Environment, 29*(5), 1576-1590. https://doi.org/10.1007/s10924-020-01977-4

[55] Almasian, A., Fard, G. C., Gashti, M. P., Mirjalili, M., & Shourijeh, Z. M. (2016). Surface modification of electrospun PAN nanofibers by amine compounds for adsorption of anionic dyes. *Desalination and Water Treatment, 57*(22), 10333-10348. https://doi.org/10.1080/19443994.2015.1041161

[56] Almasian, A., Olya, M. E., & Mahmoodi, N. M. (2015). Synthesis of polyacrylonitrile/polyamidoamine composite nanofibers using electrospinning technique and their dye removal capacity. *Journal of the Taiwan Institute of Chemical Engineers, 49*, 119-128. https://doi.org/10.1016/j.jtice.2014.11.027

[57] Mokhtari-Shourijeh, Z., Langari, S., Montazerghaem, L., & Mahmoodi, N. M. (2020). Synthesis of porous aminated PAN/PVDF composite nanofibers by electrospinning: Characterization and Direct Red 23 removal. *Journal of Environmental Chemical Engineering, 8*(4), 103876. https://doi.org/10.1016/j.jece.2020.103876

[58] Sun, Y., Luo, S., Xing, J., Li, Z., & Meng, A. (2021). Facile Synthesis of Fe/Cr-Codoped ZnO Nanoparticles with Excellent Adsorption Performance for Various Pollutants. *Journal of Ocean University of China, 20*(2), 349-360. https://doi.org/10.1007/s11802-021-4611-9

[59] Mahmoodi, N. M., Mokhtari-Shourijeh, Z., & Ghane-Karade, A. (2017). Dye removal from wastewater by the cross-linked blend nanofiber and homogenous surface diffusion modeling. *Environmental Progress & Sustainable Energy, 36*(6), 1634-1642. https://doi.org/10.1002/ep.12617

[60] Kasperiski, F. M., Lima, E. C., Reis, G. S. d., da Costa, J. B., Dotto, G. L., Dias, S. L., Cunha, M. R., Pavan, F. A., & Correa, C. S. (2018). Preparation of CTAB-functionalized aqai stalk and its efficient application as adsorbent for the removal of Direct Blue 15 and Direct Red 23 dyes from aqueous media. *Chemical Engineering Communications, 205*(10), 1520-1536. https://doi.org/10.1080/00986445.2018.1458028

[61] Coppola, G., Bhattacharyya, S., Pugliese, V., Algieri, C., Petrosino, F., Siciliano, S., & Calabro, V. (2024). Metal–organic framework application in wastewater treatment: a review. *Euro-Mediterranean Journal for Environmental Integration, 9*(1), 153-167. https://doi.org/10.1007/s41207-023-00411-0

[62] Mahmoodi, N. M., Mokhtari-Shourijeh, Z., & Ghane-Karade, A. (2017). Synthesis of the modified nanofiber as a nanoadsorbent and its dye removal ability from water: Isotherm, kinetic and thermodynamic. *Water Science and Technology, 75*(10), 2475-2487. https://doi.org/10.2166/wst.2017.022

[63] Mahvi, A. H., & Dalvand, A. (2020). Kinetic and equilibrium studies on the adsorption of Direct Red 23 dye from aqueous solution using montmorillonite nanoclay. *Water Quality Research Journal, 55*(2), 132-144. https://doi.org/10.2166/wqrj.2019.008

[64] Liu, N., Wang, H., Weng, C.-H., & Hwang, C.-C. (2018). Adsorption characteristics of Direct Red 23 azo dye onto powdered tourmaline. *Arabian Journal of Chemistry, 11*(8), 1281-1291. https://doi.org/10.1016/j.arabjc.2016.04.010

[65] Abbasian, M., Jaymand, M., Niroomand, P., Farnoudian-Habibi, A., & Karaj-Abad, S. G. (2017). Grafting of aniline derivatives onto chitosan and their applications for removal of reactive dyes from industrial effluents. *International Journal of Biological Macromolecules, 95*, 393-403. https://doi.org/10.1016/j.ijbiomac.2016.11.075

[66] Mahmoodi, N. M., Maroofi, S. M., Mazarji, M., & Nabi-Bidhendi, G. (2017). Preparation of modified reduced graphene oxide nanosheet with cationic surfactant and its dye adsorption ability from colored wastewater. *Journal of Surfactants and Detergents, 20*(5), 1085-1093. https://doi.org/10.1007/s11743-017-1985-1

[67] Hebeish, A., Ramadan, M., Abdel-Halim, E., & Abo-Okeil, A. (2011). An effective adsorbent based on sawdust for removal of direct dye from aqueous solutions. *Clean Technologies and Environmental Policy, 13*(5), 713-718. https://doi.org/10.1007/s10098-010-0343-z

[68] Abbasian, M., Niroomand, P., & Jaymand, M. (2017). Cellulose/polyaniline derivatives nanocomposites: Synthesis and their performance in removal of anionic dyes from simulated industrial effluents. *Journal of Applied Polymer Science, 134*(39), 45352. https://doi.org/10.1002/app.45352

How to cite this paper:

Soleymani, R., Mohammadnezhad, B. & Hosseini, S. A. (2026). Metal-organic framework based on iron doping: Green synthesis and sustainable adsorbent for anionic dye contaminated water. Advances in Environmental Technology, 12(3), 256-273. DOI: 10.22104/aet.2026.7493.2087